BACKSCATTERING OF ELECTRICALLY LARGE PERFECT CONDUCTING TARGETS MODELED BY NURBS SURFACES IN HALF-SPACE

X. J. Chen and X. W. Shi

National Key Laboratory of Antennas and Microwave Technology
Xidian University
Xi'an 710071, Shaanxi, China

Abstract—Backscattering Radar Cross Section (RCS) of electrically large targets is analyzed using Physical Optics (PO) approximation. The targets are located in a dielectric half-space, and modeled with Nonuniform Rational B-spline (NURBS) surfaces. The influence of the half-space is considered by the "four-path" model approximation. Results show the validity of the method.

1. INTRODUCTION

The use of Nonuniform Rational B-spline (NURBS) to describe complex targets for Radar Cross Section (RCS) computation was firstly introduced by some Spanish researchers [1, 2]. Compared with flat facets, NURBS surfaces have great advantages [1], so more and more targets are modeled with NURBS surfaces [3–7]. But, the research on NURBS model is mostly focused on the targets located in free space. For some kind of objects, such as warship on sea or tank on ground, the influence of dielectric half-space to their scattering mechanism can not be ignored. So, the author analyzed the NURBS model located in a dielectric half-space.

Although Moment Method (MOM) combined with the half-space Green's function has been proposed by many references [8–11], it is not applicable because of the mass storage memory and low computational efficiency. The "four-path" model method [12–14] is a simple, effective and efficient way to approximate the influence of the half space to the scattering mechanisms. And Physical Optics (PO) [1, 3, 6, 15] approximation is a high frequency method which is applied to calculate the RCS of electrically large targets. The method of the "four-path" model combined with PO [16] has been presented to compute the RCS

of flat plates in half space and this method can be extended to calculate the RCS of complex targets which are modeled by a series of flat plates. In this paper, the author introduced the combined method into the computation of half space NURBS model. The examples in this paper show the validity of the method.

2. NURBS TECHNIQUE

NURBS technique [17] allows a complex target to be represented with a small number of patches, for example, a cylinder or a sphere can be modeled exactly with a single NURBS surface. Therefore, it will reduce the computation time needed to analyze a realistic target. NURBS surfaces are usually transformed into Beizer patches for computation, because they are more suitable for the numerical treatment, thanks to the characteristics of the Bernstein polynomial that define the patches. The transformation of NURBS into Bezier surfaces is performed by applying the Cox-de-Boor algorithm [17]. The surface point of a Bezier surface is expressed as:

$$\overline{r}(u,v) = \frac{\displaystyle\sum_{i=0}^{m}\sum_{j=0}^{n} w_{ij}\overline{b}_{ij}B_i^m(u)B_j^n(v)}{\displaystyle\sum_{i=0}^{m}\sum_{j=0}^{n} w_{ij}B_i^m(u)B_j^n(v)}, \quad u \in (0,1),\ v \in (0,1) \qquad (1)$$

Where $\overline{b}_{ij}$ are the control points, w_{ij} are the associated weights, m and n are the surface degrees, and $B_j^n(t)$ are the Bernstein polynomials which are defined as:

$$B_j^n(t) = \left(\begin{array}{c} n \\ j \end{array}\right)(1-t)^{n-j}t^j \qquad (2)$$

3. BACKSCATTERING FIELD OF A BEZIER SURFACE LOCATED IN HALF SPACE

The scattering mechanisms considered in the approximate four-path model are illustrated in Fig. 1. When the surface of half space is assumed to lie at the $z = 0$ plane, given an incident planar wave, under the "four-path" modal approximation, the backscattered field of
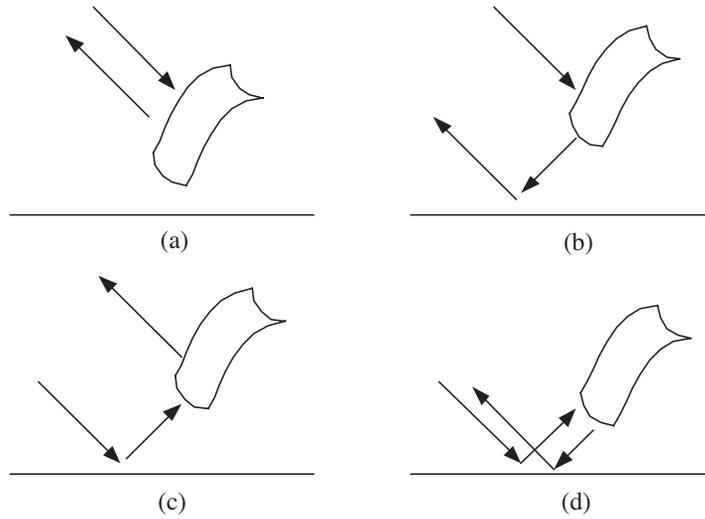
Figure 1. Scattering mechanisms of the "four-path" model. (a) Path 1. (b) Path 2. (c) Path 3. (d) Path 4.

an arbitrary conducting body predicted by PO is given by [16]:

$$\hat{e} \cdot \bar{E}_s(\bar{r}) = E_0 \frac{jk}{2\pi} \frac{e^{-jkr}}{r} \left[I(\hat{r}, 2\hat{r}) + \left\{ \begin{array}{l} R_H I(\hat{r}, \hat{r} + \hat{r}_r) + \\ R_V I(\hat{r}_r, \hat{r} + \hat{r}_r) + \end{array} \right\} \right.$$
$$\left. + \left\{ \begin{array}{l} R_H I'(\hat{r}_r \cdot \hat{n}, \hat{r} + \hat{r}_r) \\ R_V I'(\hat{r} \cdot \hat{n}, \hat{r} + \hat{r}_r) \end{array} \right\} + \left\{ \begin{array}{l} R_H^2 \\ R_V^2 \end{array} \right\} I'(\hat{r}_r \cdot \hat{n}, 2\hat{r}_r) \right] \quad (3)$$

where, $\hat{r}_r = \hat{r} - 2\hat{z}(\hat{r} \cdot \hat{z})$ is the reflected vector, k is the wave number, R_H and R_V are the Fresnel reflection coefficients for horizontal and vertical polarization respectively, which are given by:

$$R_H = \frac{\cos\theta - \sqrt{\varepsilon_r - j\sigma\dfrac{\eta_0}{k} - \sin^2\theta}}{\cos\theta + \sqrt{\varepsilon_r - j\sigma\dfrac{\eta_0}{k} - \sin^2\theta}} \quad (4)$$

$$R_V = \frac{\left(\varepsilon_r - j\sigma\dfrac{\eta_0}{k}\right)\cos\theta - \sqrt{\varepsilon_r - j\sigma\dfrac{\eta_0}{k} - \sin^2\theta}}{\left(\varepsilon_r - j\sigma\dfrac{\eta_0}{k}\right)\cos\theta + \sqrt{\varepsilon_r - j\sigma\dfrac{\eta_0}{k} - \sin^2\theta}} \quad (5)$$

ε_r and σ are the permittivity and conductivity of the half space respectively. The integral terms $I(\boldsymbol{w}, \boldsymbol{v})$ and $I'(\boldsymbol{w}, \boldsymbol{v})$ of (1) are given by:

$$I(\bar{w}, \bar{v}) = \iint\limits_{s} (\bar{w} \cdot \hat{n}) \exp(jk\bar{v} \cdot \bar{r}) dS \qquad (6)$$

$$I'(\bar{w}, \bar{v}) = \iint\limits_{s'} (\bar{w} \cdot \hat{n}) \exp(jk\bar{v} \cdot \bar{r}) dS \qquad (7)$$

where s is the illuminated portion of the incident wave, s' is the illuminated portion of the reflected wave from the surface of half-space, $\bar{r}$ is the location of an arbitrary point on the illuminated portion, $\hat{n}$ is the unit normal vector at $\bar{r}$. The integral that should be computed can be expressed on the parametric coordinates of the Bezier patch [1], so

$$I(\bar{w}, \bar{v}) = \int_0^1 \int_0^1 (\bar{w} \cdot \bar{r}_u \times \bar{r}_v) \exp(jk\bar{v} \cdot \bar{r}) du dv \qquad (8)$$

Integral (8) can be computed with the Stationary Phase Method (SPM) [1, 18]. The contribution to the integral for the doubly curved patches is given by three kinds of critical points when the SPM is applied:

1) Stationary phase points: The contributions to the integral are proportional to k^{-1} and are given by:

$$I_{sta} = \sigma \frac{2\pi \bar{w} \cdot \bar{r}_u \times \bar{r}_v}{k} \exp(jk\bar{v} \cdot \bar{r})$$
$$\sqrt{\frac{1}{\left|(\bar{v} \cdot \bar{r}_{uu})(\bar{v} \cdot \bar{r}_{vv}) - (\bar{v} \cdot \bar{r}_{uv})^2\right|}} \exp\left[j\frac{\pi}{4}\sigma(\delta + 1)\right] \quad (9)$$

where $\sigma = \operatorname{sign}(\bar{v} \cdot \bar{r}_{uu})$, and $\delta = \operatorname{sign}\left[(\bar{v} \cdot \bar{r}_{uu})(\bar{v} \cdot \bar{r}_{vv}) - (\bar{v} \cdot \bar{r}_{uv})^2\right]$

2) Boundary critical points: The contributions to the integrals which are proportional to $k^{-3/2}$ are:

$$I_{bou} = j(-1)^\alpha \frac{(\bar{w} \cdot \bar{r}_u \times \bar{r}_v)}{k\bar{v} \cdot \bar{r}_\alpha} \exp(jk\bar{v} \cdot \bar{r}) \sqrt{\frac{2\pi j}{k\bar{v} \cdot \bar{r}_{\beta\beta}}} \qquad (10)$$

where on the boundaries $u = 0$ and $u = 1$, α is u and β is v, and on the boundaries $v = 0$ and $v = 1$, α is v and β is u.

3) Vertex points: The main contributions to the integrals are proportional to k^{-2} and are given by

$$I_{ver} = -(-1)^{u+v} \frac{(\bar{w} \cdot \bar{r}_u \times \bar{r}_v)}{k^2 (\bar{v} \cdot \bar{r}_u)(\bar{v} \cdot \bar{r}_v)} \exp(jk\bar{v} \cdot \bar{r}) \qquad (11)$$

For singly curved patches, the above expressions are not valid because the second derivation of $\bar{r}(u,v)$ is equal to zero for one parametric coordinate. In this case, the integration along the linear coordinate can be calculated analytically and the SPM is applied to evaluate the integral along the other coordinate. For example, if the surface is linear with the parametric coordinate v, the PO integral can be written as:

$$I = \int_0^1 I_u(v)\, dv \qquad (12)$$

where

$$I_u = \int_0^1 (\bar{w} \cdot \bar{r}_u \times \bar{r}_v) \exp(jk\bar{v} \cdot \bar{r}) du \qquad (13)$$

The contribution to the integral is calculated by two kinds of critical segments when the SPM is applied:

1) Stationary phase segments:

$$I_{sta} = (\bar{w} \cdot \bar{r}_u \times \bar{r}_v) \exp(jk\bar{v} \cdot \bar{r}) \sqrt{\frac{2\pi j}{k\bar{v} \cdot \bar{r}_{uu}}} \qquad (14)$$

2) Boundary segments:

$$I_{bou} = j(-1)^{u_0} \exp(jk\bar{v} \cdot \bar{r}) \frac{\bar{w} \cdot \bar{r}_u \times \bar{r}_v}{k |\bar{v} \cdot \bar{r}_u|} \qquad (15)$$

These expressions are integrated analytically along the coordinate v to obtain the scattered field.

4. NUMERICAL RESULTS

The frequency of the incident planar wave is $3\,\text{GHz}$, and the relative permittivity and conductivity of the half space is $\varepsilon_r = 76.7 - j12$ and $\sigma = 4\,\text{mho/m}$ respectively. Numerical results of RCS for different geometries are presented below.
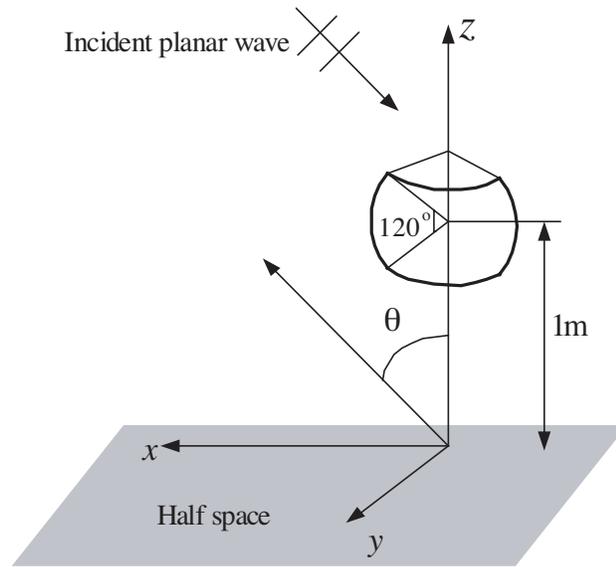
Figure 2. Geometry of a spherically curved plate.

4.1. Spherically Curved Plate

An object which is modeled with only one doubly curved Bezier surface is shown in Fig. 2. The plate extends over a beam of 120° for θ angles and 90° for φ angles. The radius of the sphere is 1 m, and the distance between the centre of the sphere and the half space surface is 1 m too. Fig. 3 show the RCS result at the $\varphi = 90°$ cut, as a function of θ angle for horizontal polarization. The result from Numerical method is obtained using numerical integration [16].

4.2. Cylindrically Curved Plate

This object is one quarter of a cylinder and is modeled with only one singly curved Bezier surface. The geometry of the plate is presented in Fig. 4. The height of the plate is 0.5 m, and the radius of the cylinder is 0.2 m. The distance between the plate and the half space surface is 0.5 m. Fig. 5 show the RCS results at $\varphi = 90°$ cut for horizontal polarization. The result from Numerical method is obtained using numerical integration [16].
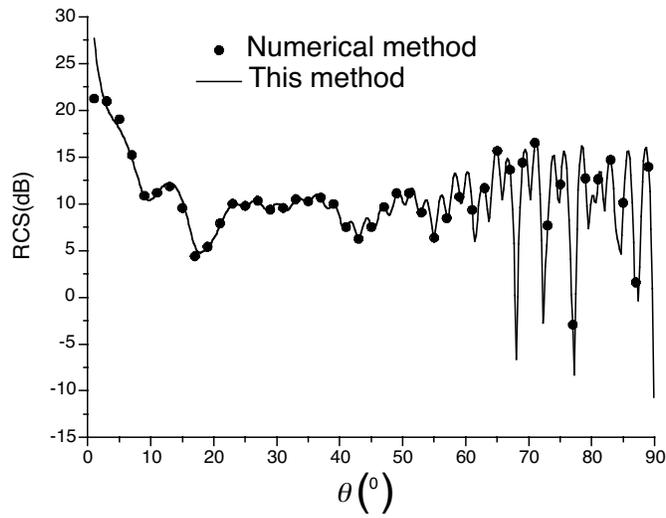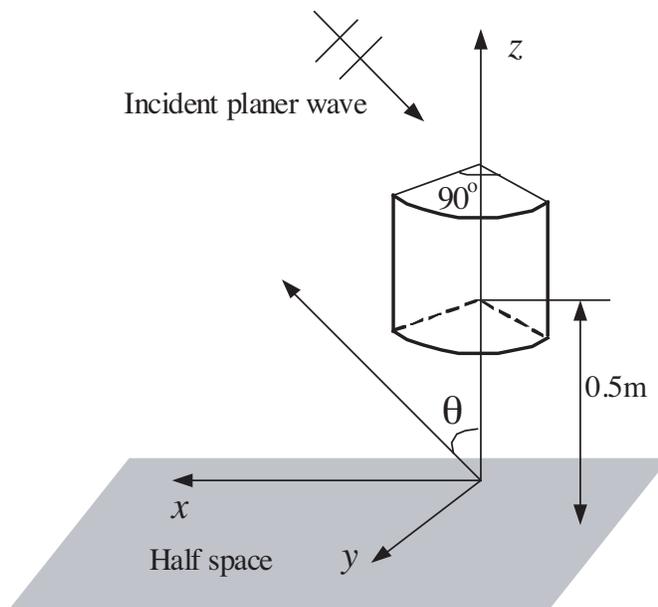
Figure 3. RCS of the spherically curved plate.

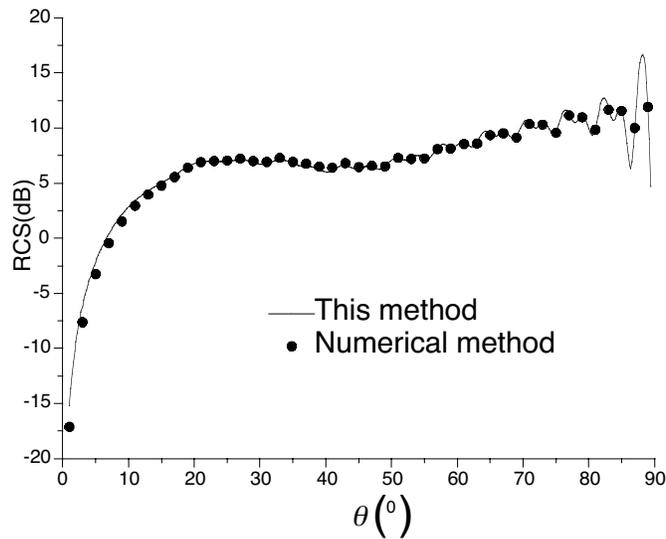**Figure 4.** Geometry of a cylindrically curved plate.

Figure 5. RCS of the cylindrically curved plate.

5. CONCLUSION

A method for the RCS computation of electrically large conducting bodies modeled with NURBS surfaces in half space is presented using PO approximation. The results from the method presented in this paper agree very well with those obtained from the numerical method, which shows that the presented method is valid.

ACKNOWLEDGMENT

REFERENCES

1. Perez, J. and M. F. Catedra, "Application of physical optics to the RCS computation of bodies modeled with NURBS surfaces," *IEEE Transactions on Antennas and Propagation*, Vol. 42, No. 10, 1404–1411, 1994.

2. Domingo, M., F. Rivas, J. Perez, and M. F. Catedra, "Computation of the RCS of complex bodies modeled using NURBS sur-

faces," *IEEE Transactions on Antennas and Propagation*, Vol. 37, No. 6, 36–47, 1995.

3. Chen, M., Y. Zhang, and C. H. Liang, "Calculation of the field distribution near electrically large NURBS surfaces with physical optics method," *Journal of Electromagnetic Waves and Applications*, Vol. 19, No. 11, 1511–1524, 2005.

4. Wang, N., Y. Zhang, and C. H. Liang, "Creeping ray-tracing algorithm of UTD method based on NURBS models with the source on surface," *Journal of Electromagnetic Wave Applications*, Vol. 20, No. 14, 1981–1990, 2006.

5. Chen, M., X. W. Zhao, Y. Zhang, and C. H. Liang, "Analysis of antenna around NURBS surface with iterative MOM-PO technique," *Journal of Electromagnetic Wave Applications*, Vol. 20, No. 12, 1967–1680, 2006.

6. Pippi, A., S. Della Case, and S. Maci, "A line-integral asymptotic representation of the PO radiation from NURBS surfaces," *Antennas and Propagation Society International Symposium, IEEE*, Vol. 4, No. 6, 4511–4514, 2004.

7. Wang, N. and C. H. Liang, "Study on the occlusions between rays and NURBS surfaces in optical methods," *Progress In Electromagnetics Research*, PIER 71, 243–249, 2007.

8. Wang, Y. and D. Longstaff, "Fast computation of Green's functions for a lossy dielectric half-space," *Microwave and Optical Technology Letters*, Vol. 25, No. 4, 287–289, 2000.

9. Sarabandi, K. and I.-S. Koh, "Fast multipole representation of Green's function for an impendance half-space," *IEEE Transactions on Antennas and Propagation*, Vol. 52, No. 1, 296–301, 2004.

10. Knockaert, L. F., "Optimizing Green's functions in grounded layered media with artificial boundary conditions," *Progress In Electromagnetics Research*, PIER 62, 69–87, 2006.

11. Xu, X. B. and Y. F. Huang, "An efficient analysis of vertical dipole antennas above a lossy halfl-space," *Progress In Electromagnetics Research*, PIER 74, 353–377, 2007.

12. Shtager, E. A., "An estimation of sea surface influence on radar reflectivity of ships," *IEEE Trans Antennas Propagate*, Vol. 47, No. 10, 1623–1627, 1999.

13. Sletten, M. A., D. B. Trizna, and J. P. Hansen, "Ultrawide-band radar observations of multipath propagation over the sea surface," *IEEE Trans Antennas Propagate*, Vol. 44, No. 5, 646–651, 1996.

14. Johnson, J. T., "A study of the four-path model for scattering from an object above a half-space," *Microwave Optical Technology Letters*, Vol. 30, No. 2, 130–134, 2001.

15. Nie, X. C., Y. B. Gan, N. Yuan, and C. F. Wang, "An efficient hybrid method for analysis of slot arrays enclosed by a large radome," *Journal of Electromagnetic Waves and Applications*, Vol. 20, No. 2, 249–264, 2006.

16. Anastassiu, H. T., "A closed form, physical optics expression for the radar cross section of a perfectly conducting flag plate over a dielectric half-space," *Radio Science*, Vol. 38, 10-1-10-13, 2003.

17. Shi, F. Z., *Computer Aided Design and Nonuniform Rational B-spline*, Peking Higher Education Publisher, 2001.

18. Jones, D. S. and M. Kline, "Asymptotic expansions of multiple integrals and the method of the stationary phase," *Journal of Mathematical Physics*, Vol. 37, 1–28, 1957.